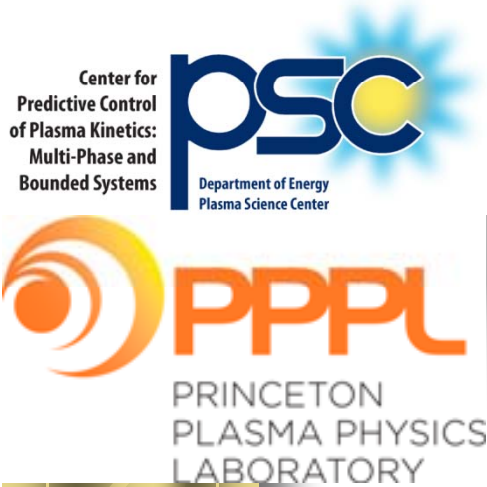


Application of Nonlocal Electron Kinetics to Plasma Technologies



Igor D. Kaganovich¹,

Dmytro Sydorenko², Alex Khrabrov¹,

Michael Campanell¹, Yevgeny Raitses¹,

Vladimir I. Demidov³, Irina Schweigert⁴,

and Alexander S. Mustafaev⁵

¹*Princeton Plasma Physics Laboratory, NJ, USA*

²*University of Alberta, Canada*

³*AFRL, Wright-Patterson, OH, USA*

⁴*ITAM, Novosibirsk, Russia*

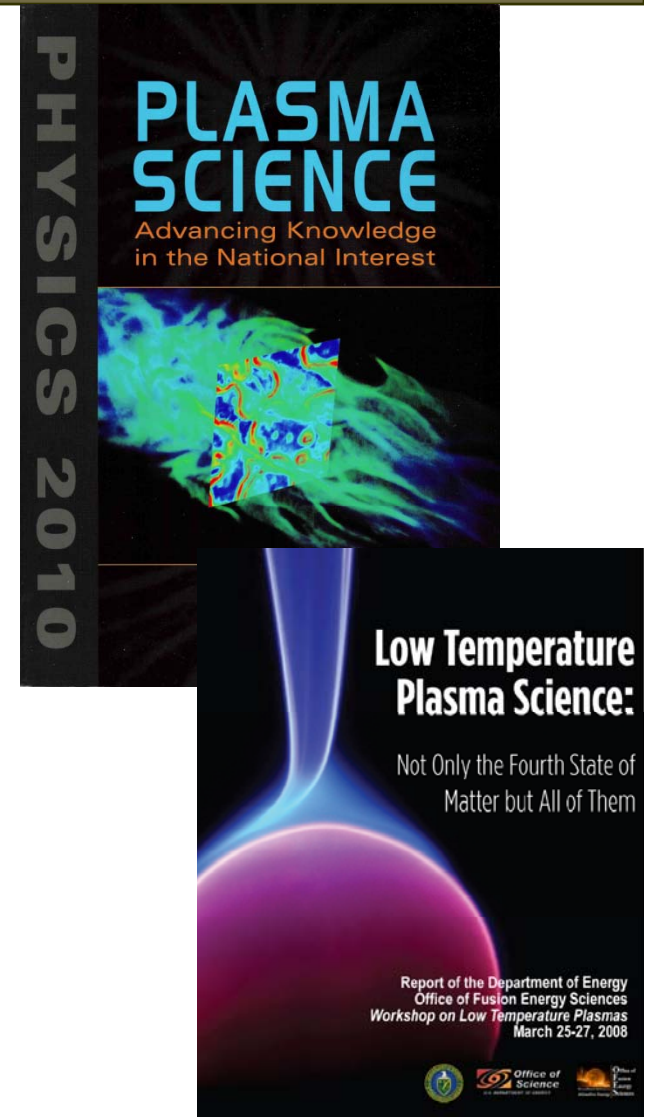
⁵*Minining Institute, St. Petersburg, Russia*

Department of Energy endorsed recommendations

- National Academies Plasma 2010 Decadal Study “Plasma Science Advancing Knowledge in the National Interest.”
- Report on Scientific Directions for Low Temperature Plasma sponsored by Department of Energy

Highest Priority Recommendation:

Development of methods to predictably control distributions functions of electrons, ions, photons



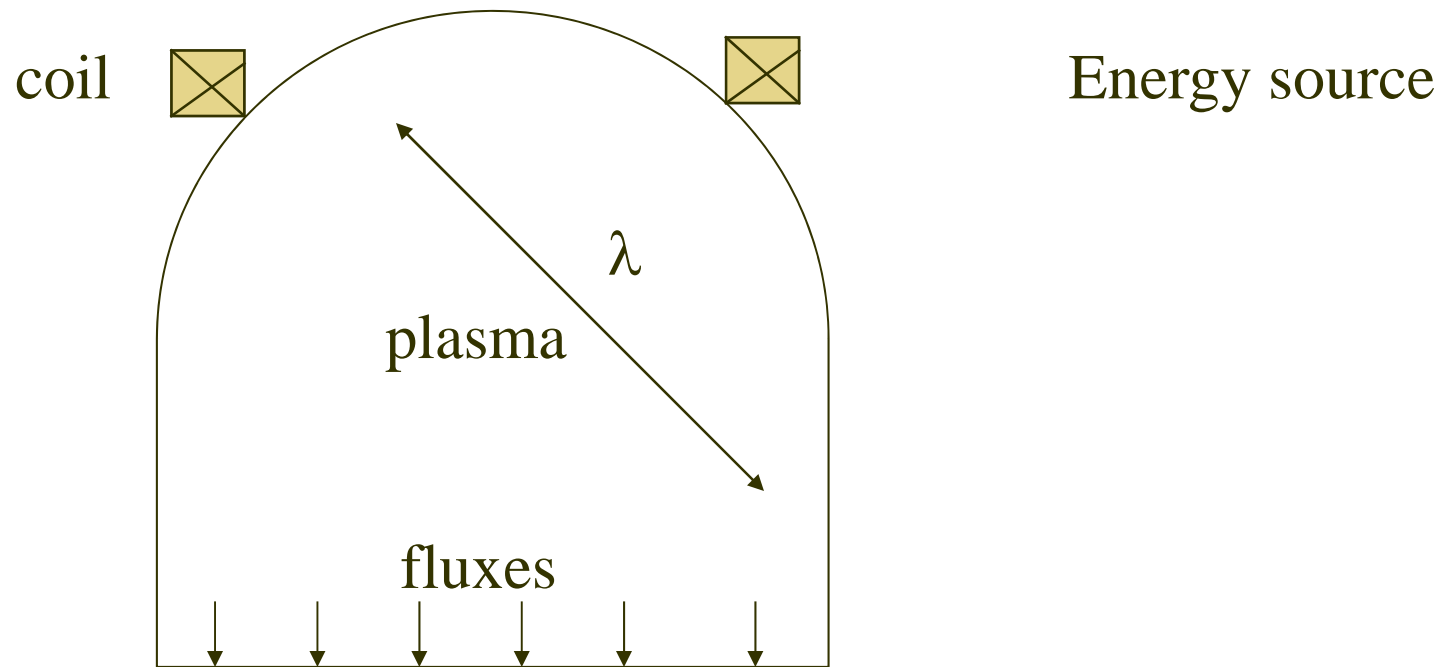
Outline: Examples of strong nonlocal electron kinetic effects not captured in fluid models:

- Explosive generation of cold electrons with power increase.
- Strong modification of electron energy distributions due to bounce resonance effect.
- Formation of anisotropic EVDF.
- Collective stopping and scattering of electron beams emitted from the walls.

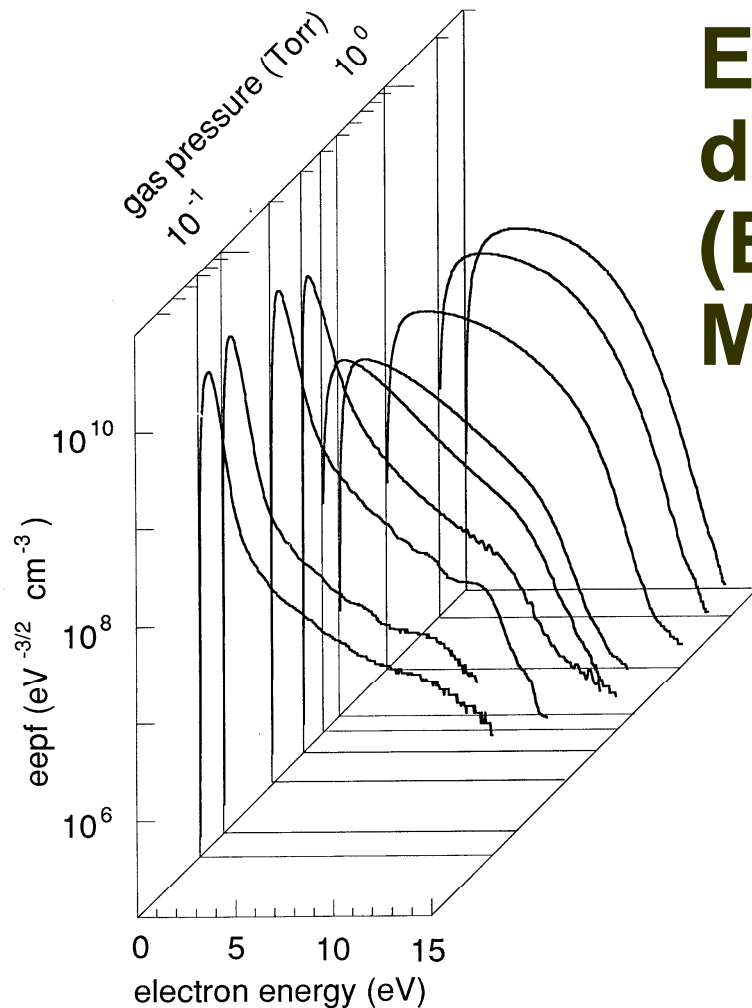
Applications: rf and dc discharges for plasma processing and electric propulsion.

Nonlocality is not just for academic interests but foundation of most plasma applications

Electron energy relaxation length is large; this allows *remote* plasma handling via nonlocal electron energy distribution function (EEDF).



Discharge modeling needs to be kinetic!



Electron energy distribution functions (EEDF) are non-Maxwellian:

- **Parts of the EEDF are very flexible and almost independent.**
- **An example of a EEDF in capacitive discharge.**

For more info:

V. Godyak, IEEE TPS 34, 755 (2006).

Discharge modeling needs to be nonlinear!

Strong coupling between plasma density, electric field profile through ionization and transport.

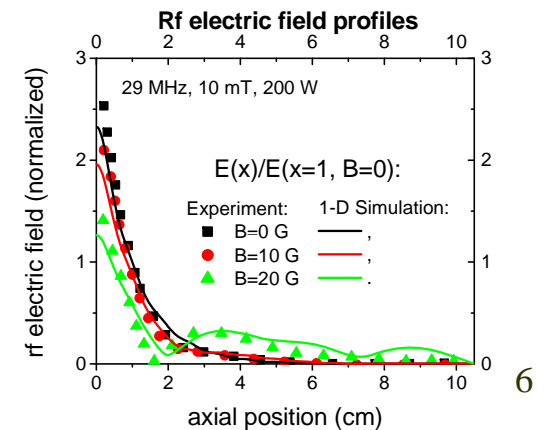
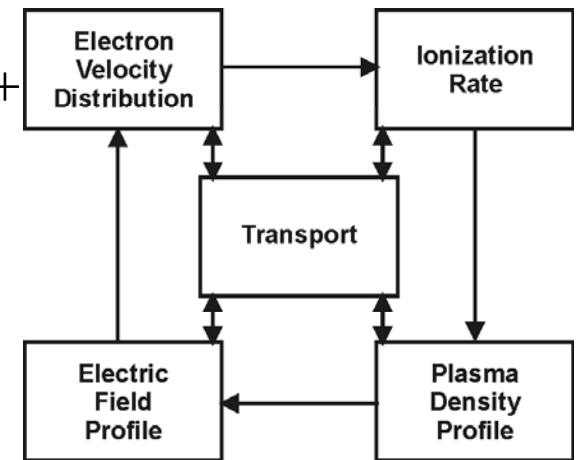
Mostly due to strong dependence of number of fast electrons on plasma parameters.

$$\left[\frac{\partial}{\partial t} + (\mathbf{v} \cdot \nabla) - e\mathbf{E} \frac{\partial}{m\partial \mathbf{v}} \right] f_0 = \sum_k \left[v_k^* \frac{\sqrt{u'}}{\sqrt{u}} f_0 (\varepsilon + \varepsilon_k^*) - \overline{v_k^*} f_0 \right] +$$

$$\frac{\partial n_i}{\partial t} + \nabla \cdot (\mathbf{v} n_i) = v_{iz} n_i, v_{iz} n_i = \int_I f_0(u) v \sigma_{iz} dv$$

$$\nabla \cdot \mathbf{E} = 4\pi e(n_i - n_e)$$

$$M_i \left(\frac{\partial \mathbf{v}}{\partial t} + (\mathbf{v} \cdot \nabla) \mathbf{v} \right) = e\mathbf{E} - \frac{\nabla p_i}{n_i} - (v_{ia} + v_{iz}) \mathbf{v}$$



I.D. Kaganovich *et al*, Phys. Rev. Lett. 1999, 2000, 2002; V.A. Godyak, *et al*, Phys. Rev. Lett. 1990, 1992, 1996, 1998, 1999 + many others.

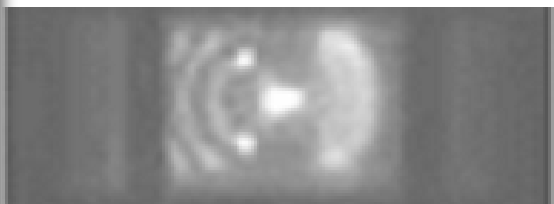
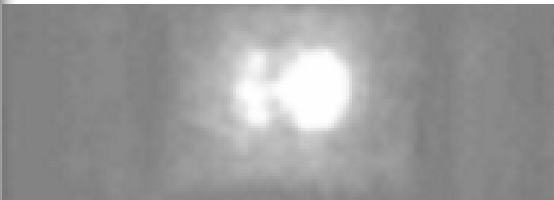
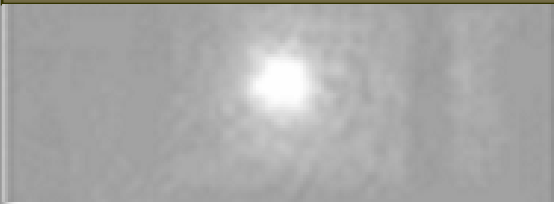
PDP discharge phases

experiment

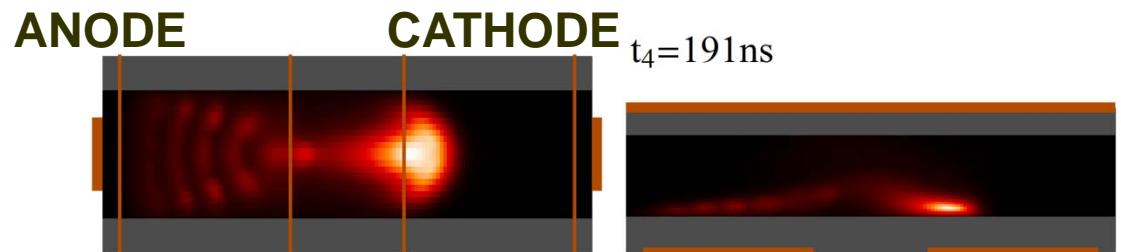
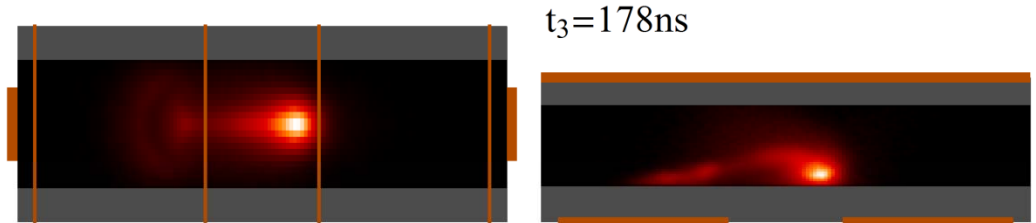
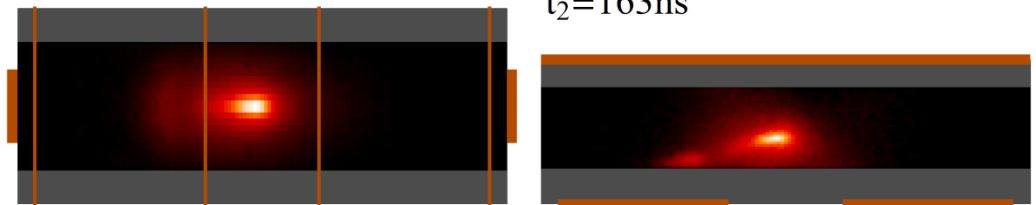
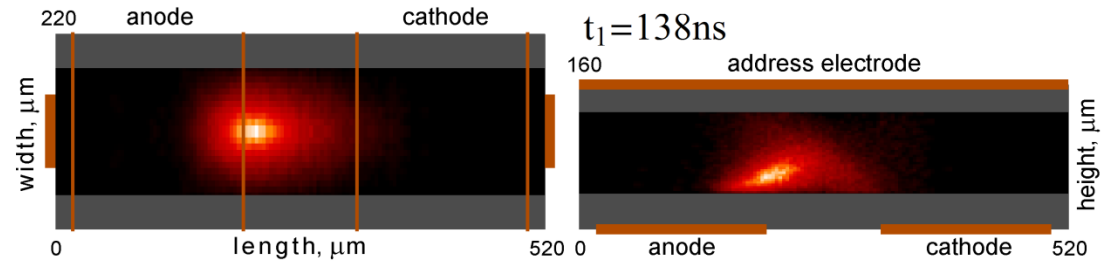
PIC simulations

Top view

Side view



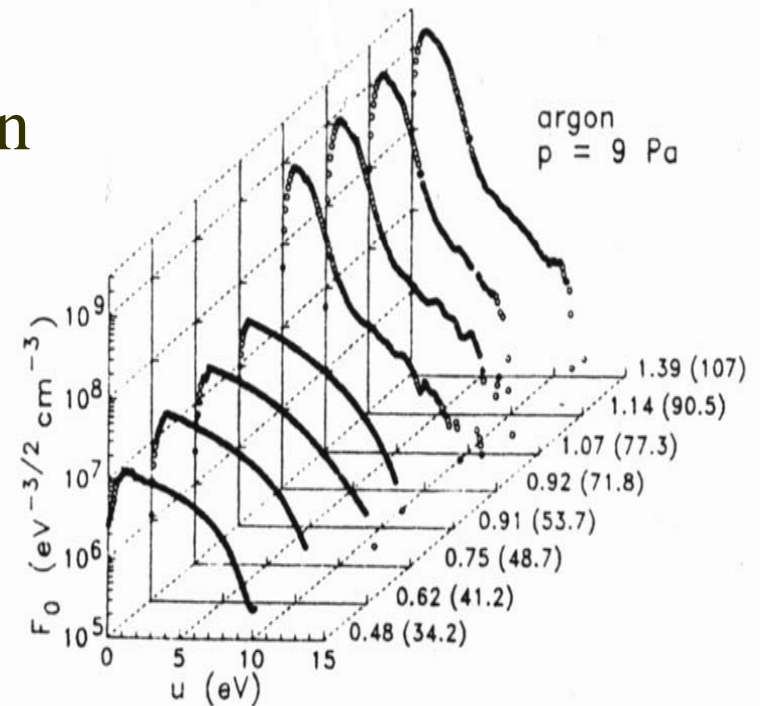
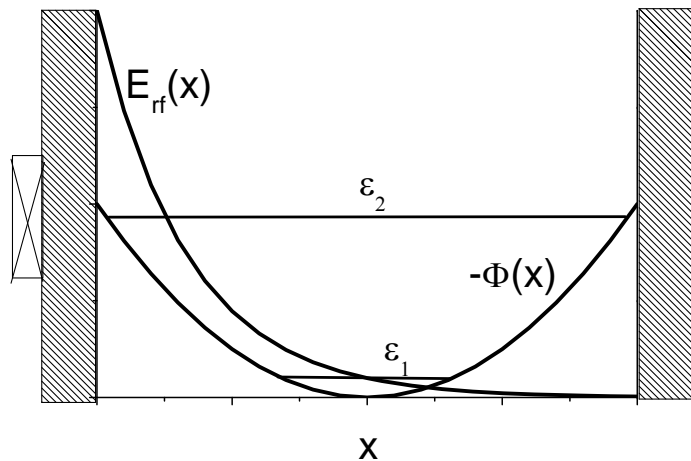
V. N. Khudik, A. Shvydky,
V. P. Nagorny, and C.E.
Theodosiou, *IEEE Trans
Plasma Sci.* **33**, 510 (2005).



Explosive generation of cold electrons with power increase (1/3)

EDF evolution with current
capacitively coupled discharge in
Argon, 13.56MHz, 6cm, 9Pa

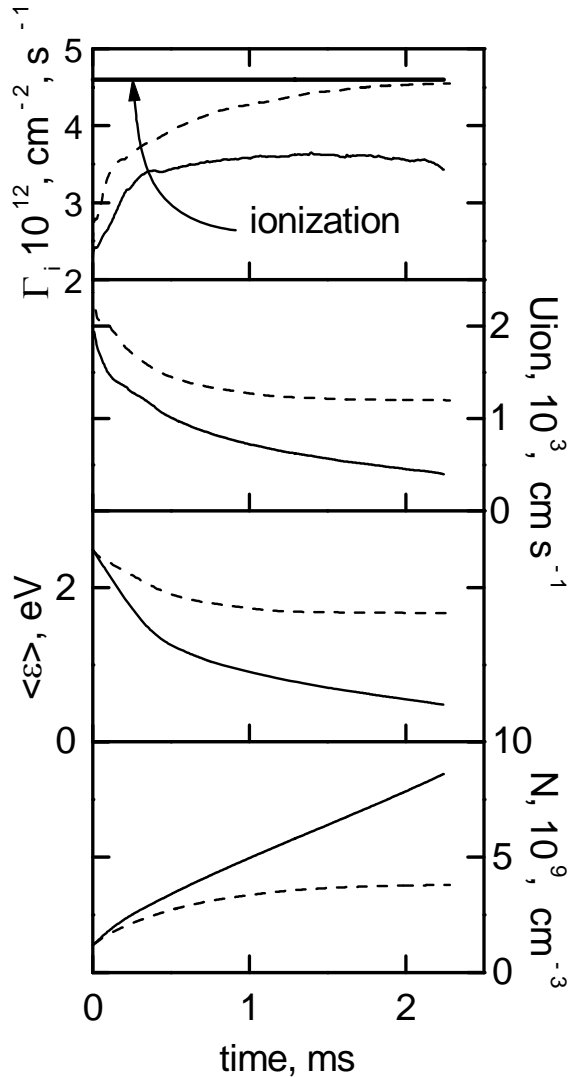
U. Buddemeier et.al. APL (1996)



$$n \uparrow \quad E \downarrow \quad T_e \downarrow$$

Cold electrons are trapped in region of weak electric field =>
density increase with given current leads to cooling

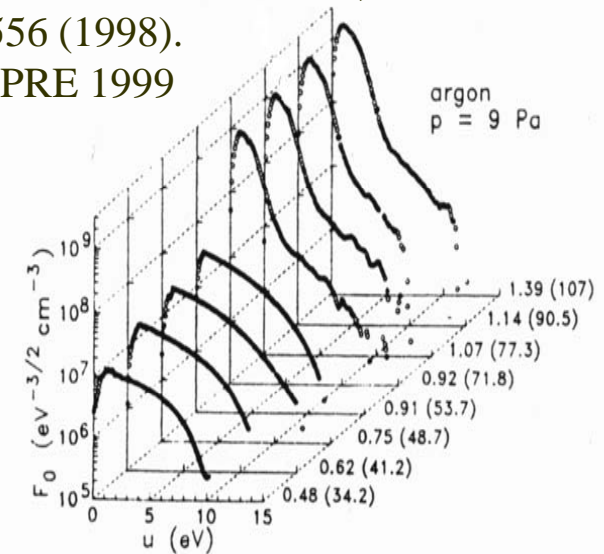
Explosive generation of cold electrons with power increase (2/3)



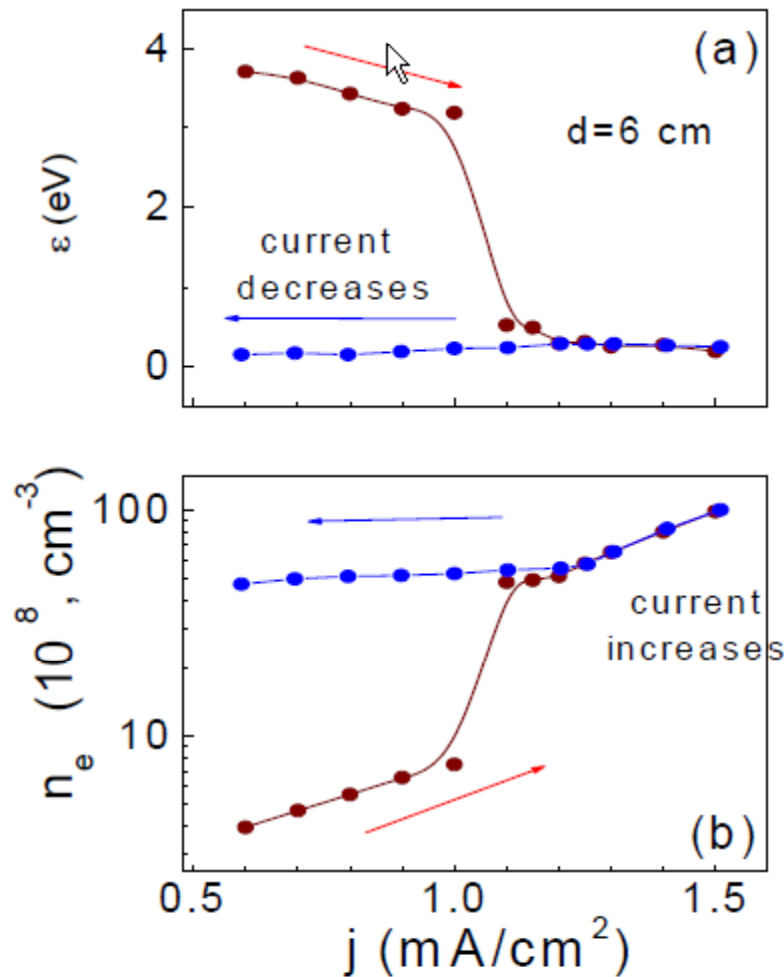
$$n \uparrow \quad T_e \downarrow \quad U_i \downarrow \quad \Gamma_i = nU_i \text{ saturates}$$

In plasma temporal evolution to steady state if ion flux does not grow with density the density explosively grows until ion flux match ionization source.

S.V. Berezhnoi, I.D. Kaganovich and L.D. Tsendin,
 Plasma Physics Reports **24**, 556 (1998).
 For ECR I. Kaganovich et.al. PRE 1999



Explosive generation of cold electrons with power increase (2/3)

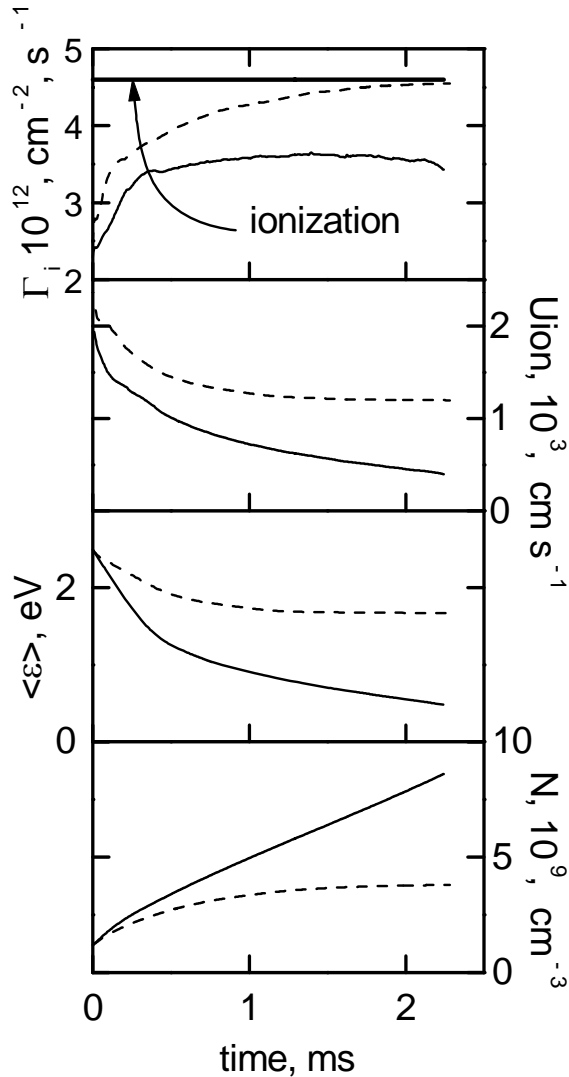


I.V. Schweigert, “*Different Modes of a Capacitively Coupled Radio-Frequency Discharge in Methane*”, Phys. Rev. Lett. 92, 155001(2004).

The electron energy and density as function of current for P 0.075 Torr and $d=6$ cm.

The transition between two modes of the discharge have been shown to be not related to the α - γ transition in discharge. The hysteresis in the discharge behavior was observed.

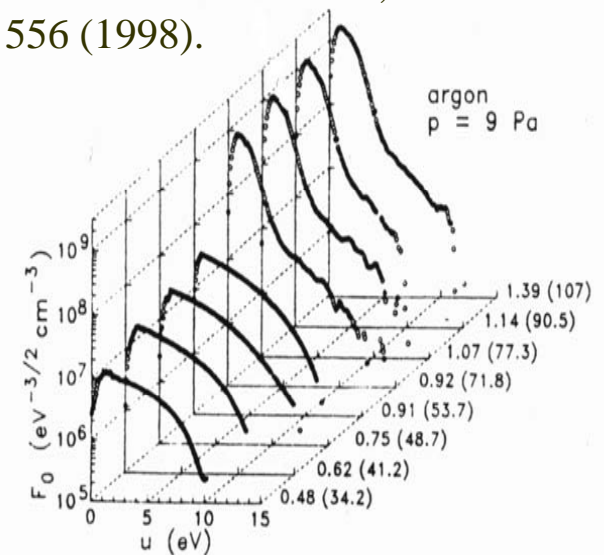
Explosive generation of cold electrons with power increase (2/3)



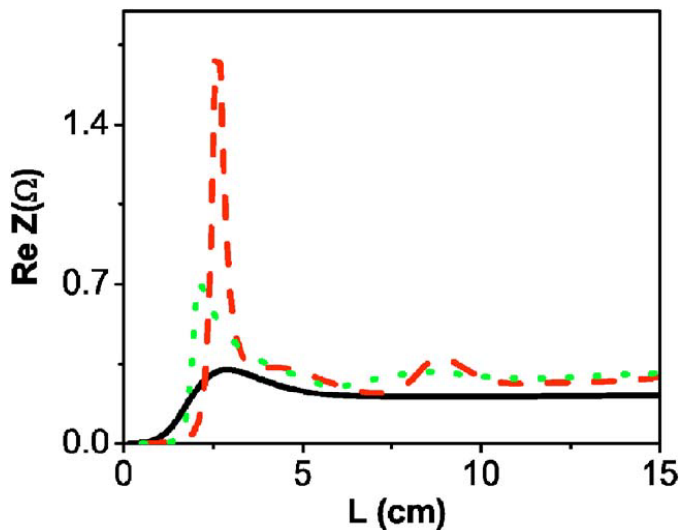
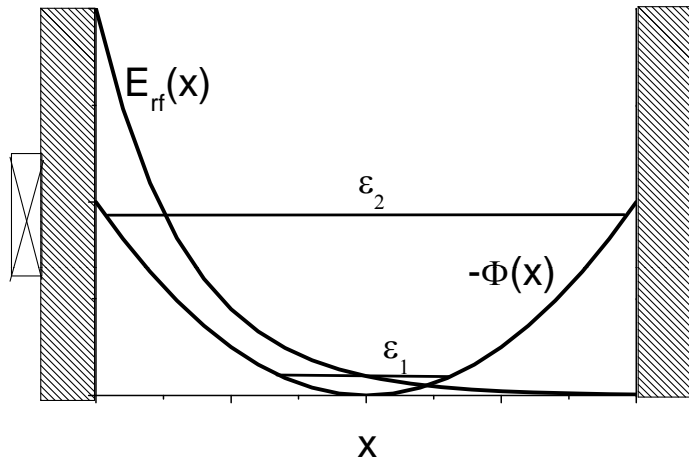
$$n \uparrow \quad T_e \downarrow \quad U_i \downarrow \quad \Gamma_i = nU_i \text{ saturates}$$

In plasma temporal evolution to steady state if ion flux does not grow with density the density explosively grows until ion flux match ionization source.

S.V. Berezhnoi, I.D. Kaganovich and L.D. Tsendin, Plasma Physics Reports **24**, 556 (1998).



Strong modification of electron energy distributions due to bounce resonance effect (1/2)



Electron interaction is most effective when bounce resonance exist: frequency of the applied wave match the frequency of the bouncing in the potential well. $f=1/T$
T is the bounce period of electron motion in the potential well.

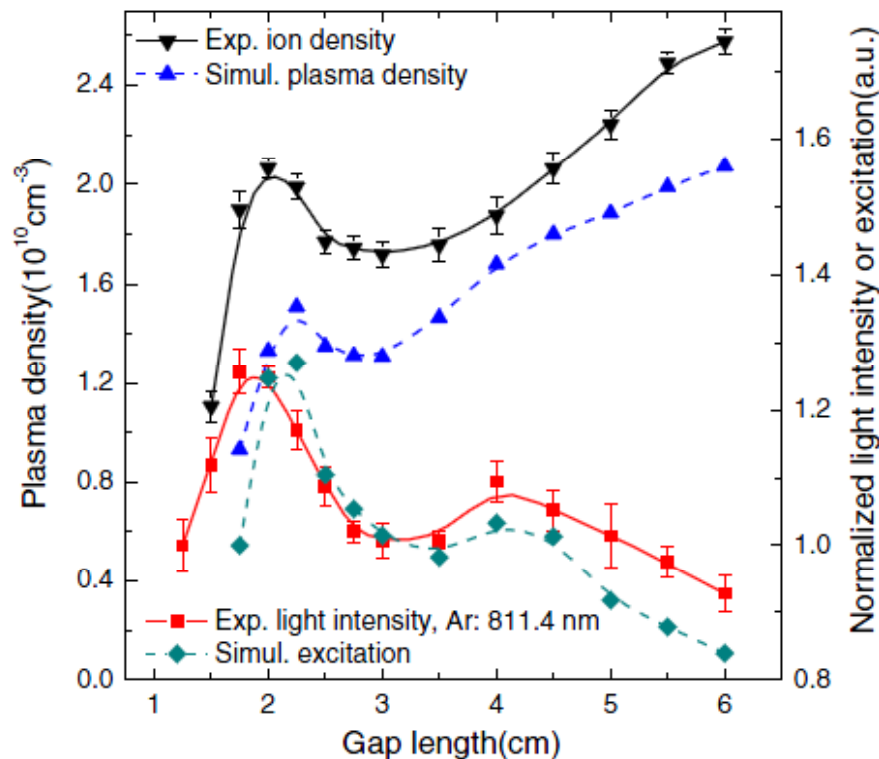
\Rightarrow Plasma resistivity depends on discharge length, L.

Oleg V. Polomarov, et al., PoP **12**, 080704 (2005).

Strong modification of electron energy distributions due to bounce resonance effect (2/2)

Discharge can be optimized by choosing bounce resonance condition for effectively heating “useful” electrons.

Yong-Xin Liu, et al., Collisionless Bounce Resonance Heating in Dual-Frequency Capacitively Coupled Plasmas, PRL 107, 055002 (2011) .

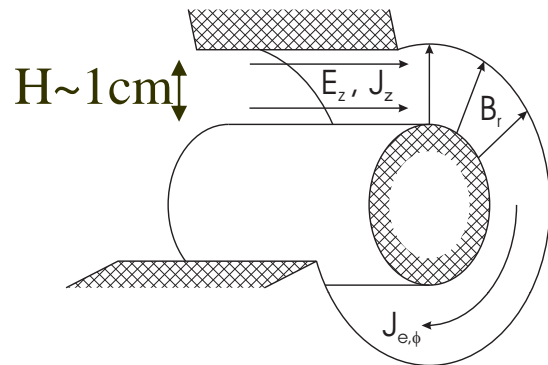


Plasma density and light intensity versus L , both measured at the center of the discharge gap at a fixed power. Solid lines are experimental measurements at 0.7 Pa, while dashed lines are simulations at 1.3 Pa. Dual frequency CCP, low frequency 1.5 to 2.5 MHz, power from 0 to 150W, the high frequency and power are fixed at 60 MHz and 50 W.

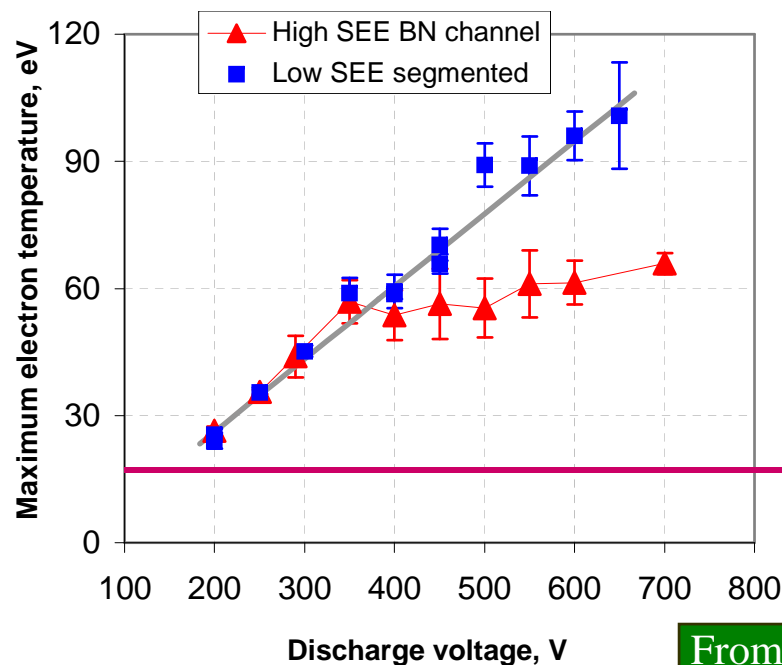
Formation of anisotropic EVDF

- Achievements of the nanoelectronics of future will largely depend on progress in creating effective anisotropic plasma reactors for the development of trillions one-electron transistors, with dimensions of 5 nm to 2024.
- A modern reactors of isotropic plasma does not allow to reach that size. To solve this problem can only use the reactors with anisotropic plasma*.
- *M. Lieberman, “Plasma Processing for Nanoelectronics - History and Prospects”, *Bull. APS, 2010, V. 55, №7, P. 105 (7th ICRP & 63th GEC, 2010, Paris, France)*.
- *Because scattering cross section is comparable to ionization cross section for energies 50-200eV, the anisotropy can be achieved is plasma is collisionless or beam has high energy $\gg 200\text{eV}$.*

Formation of anisotropic EVDF in Hall thruster



$B \sim 100\text{G}$, $E \sim 100\text{V/cm}$, $T_e \sim 100\text{eV}$.
 $P=0.1\text{-}1\text{mTorr}$, the plasma inside the thruster channel is collisionless,
 $\lambda_{ec} (\sim 1\text{m}) \gg H (\sim 1\text{cm})$. \Rightarrow intense particle and heat wall losses!



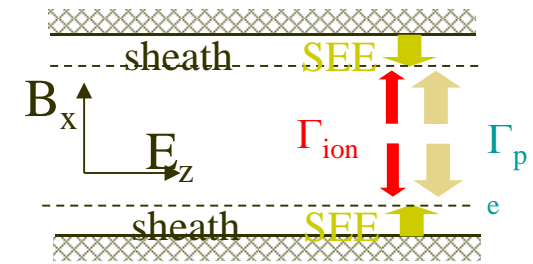
High electron temperature is observed in experiments

- *Large quantitative disagreement with fluid theories.*

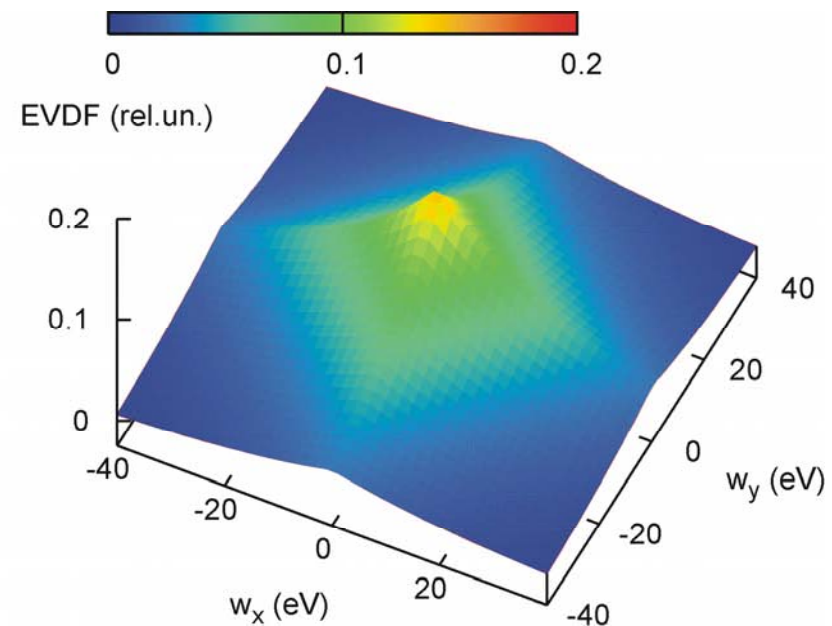
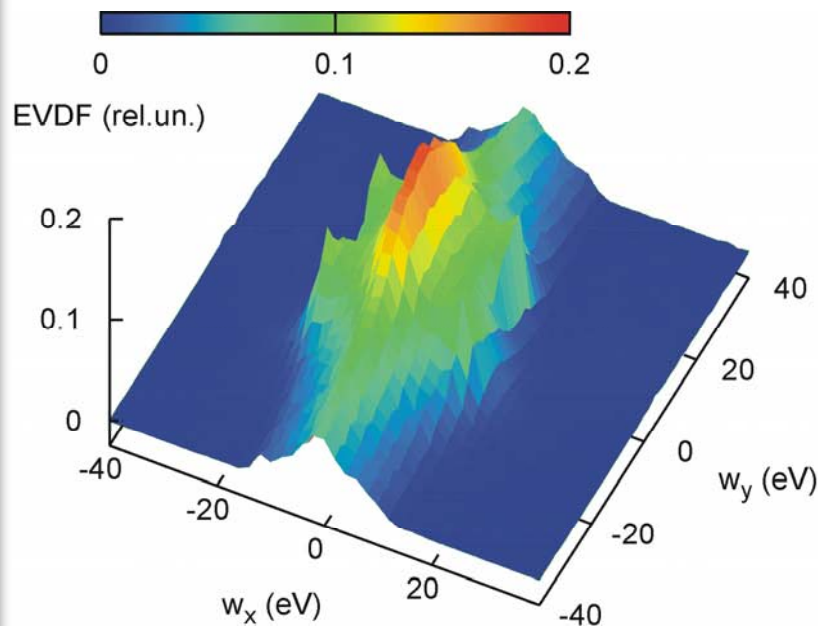
A fluid theory prediction.

From: Y. Raitses, et al., Phys. Plasmas **13**, 014502 2006.

Particle-in-cell simulations of collisionless Hall thruster plasma



Complex structure of strongly anisotropic electron velocity distribution function (EVDF) in the channel of a Hall thruster discharge (left) versus an isotropic Maxwellian EVDF (right).



=> Completely different implications follow from kinetic or fluid description for the Hall thruster operation.

High-energy electrons leave quickly, the EVDF is depleted => wall flux is small.

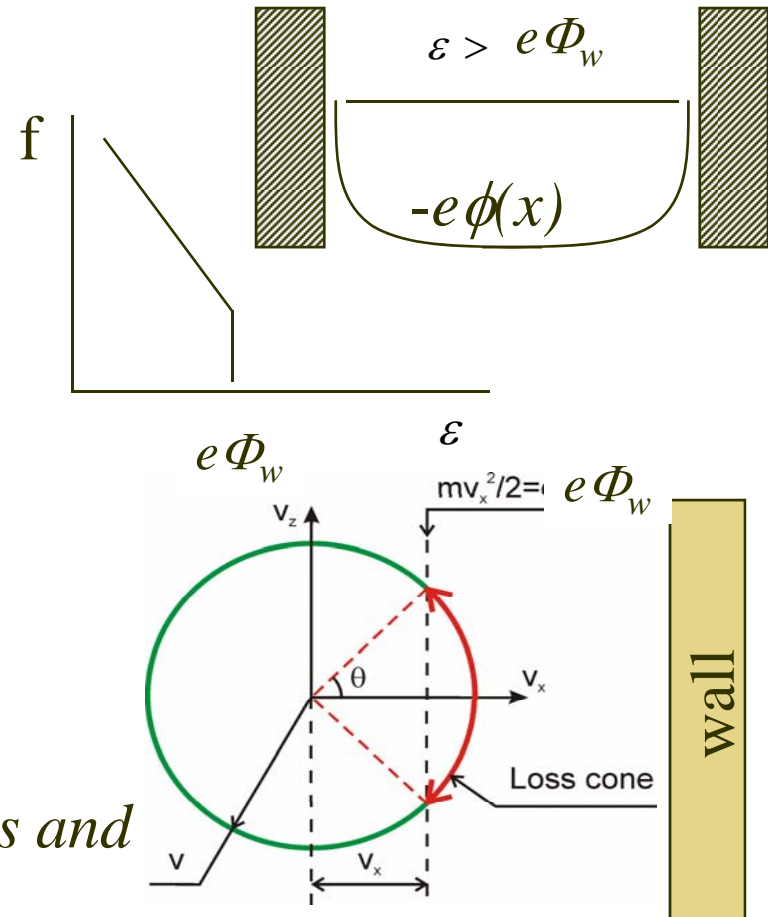
Most electrons are trapped in the potential well.

Electrons with $\varepsilon > e\Phi_w$ leave.

Electron scattering due to elastic collisions with atoms governs the electron wall fluxes.

$$\Gamma_e = \left(\frac{H}{8\lambda_c} \right) n_e \sqrt{\frac{8T_{ez}}{\pi m}} \exp\left(-\frac{\Phi_w}{T_{ez}} \right)$$

Wall flux is 1/100 of the fluid predictions and wall potential is $\sim 1T_e/e$ instead of $5T_e/e$.



See:

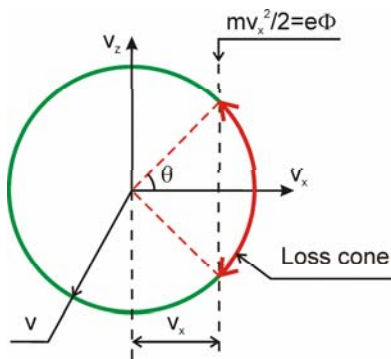
D. Sydorenko et al 8 papers in PRL, PoP, IEEE TPS

Reasons for the EVDF anisotropy

$v_{en} \tau \sim 1$ – electrons undergo few collisions with atoms before escaping to the walls.

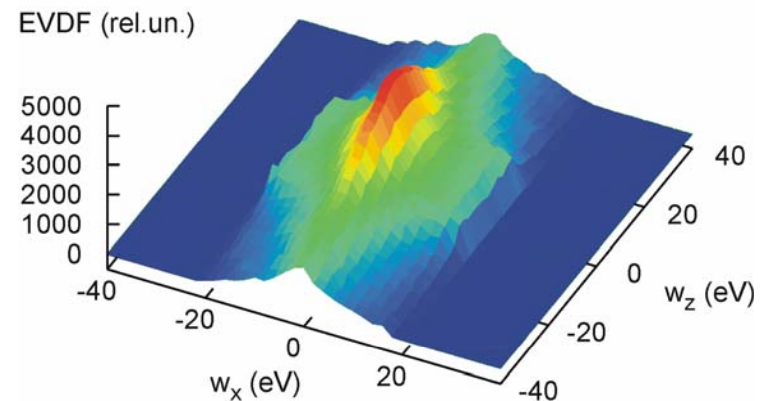
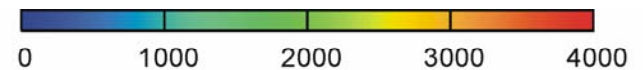
$v_{iz} \sim v_{en}$ - Xenon inelastic cross sections are large.

Consequence: $T_x < T_z$ and $v_T \sim u_d$.



$E_z = 200 \text{ V/cm}$, $B_x = 100 \text{ G}$

$T_x = 12 \text{ eV}$, $T_z = 37 \text{ eV}$!

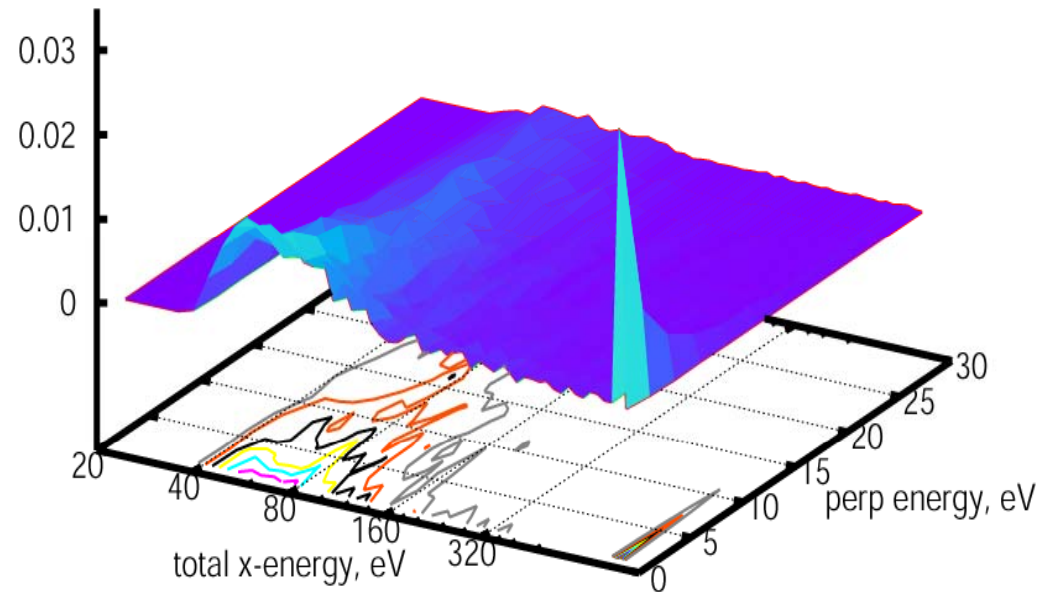
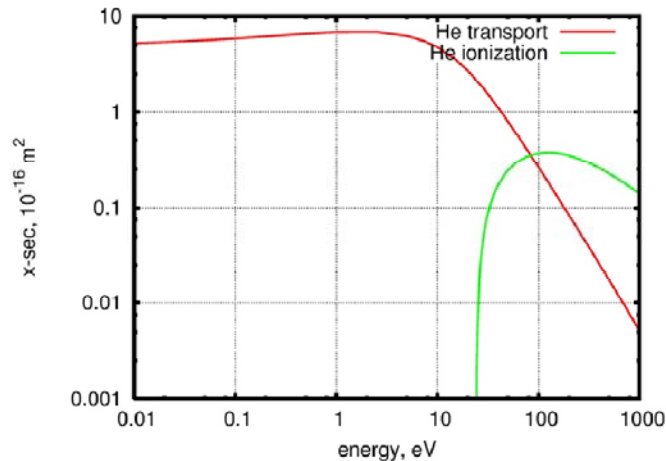
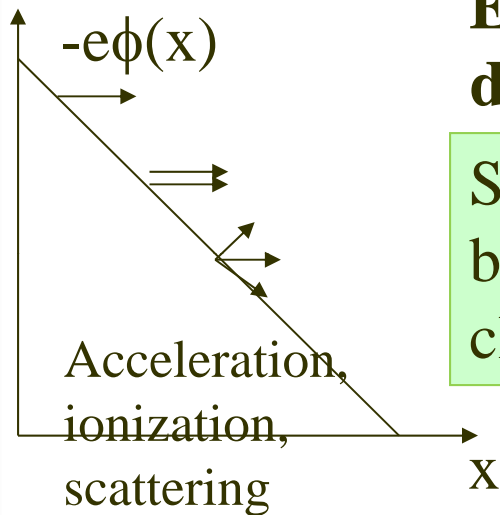


The wall potential in Hall thrusters is small, $e\Phi_w \sim T_e \Rightarrow$ The frequency of electrons leaving the plasma is the same as the frequency of electron scattering off neutrals.

Anisotropic velocity distribution in the cathode fall, showing the primary beam and the avalanche

EVDF as a function of total energy in dc discharge, 3Torr He, 800V, 1.2 cm gap

Secondary electrons scatter as they accelerate, but their distribution remains anisotropic with clear evidence of the beam emitted from cathode.

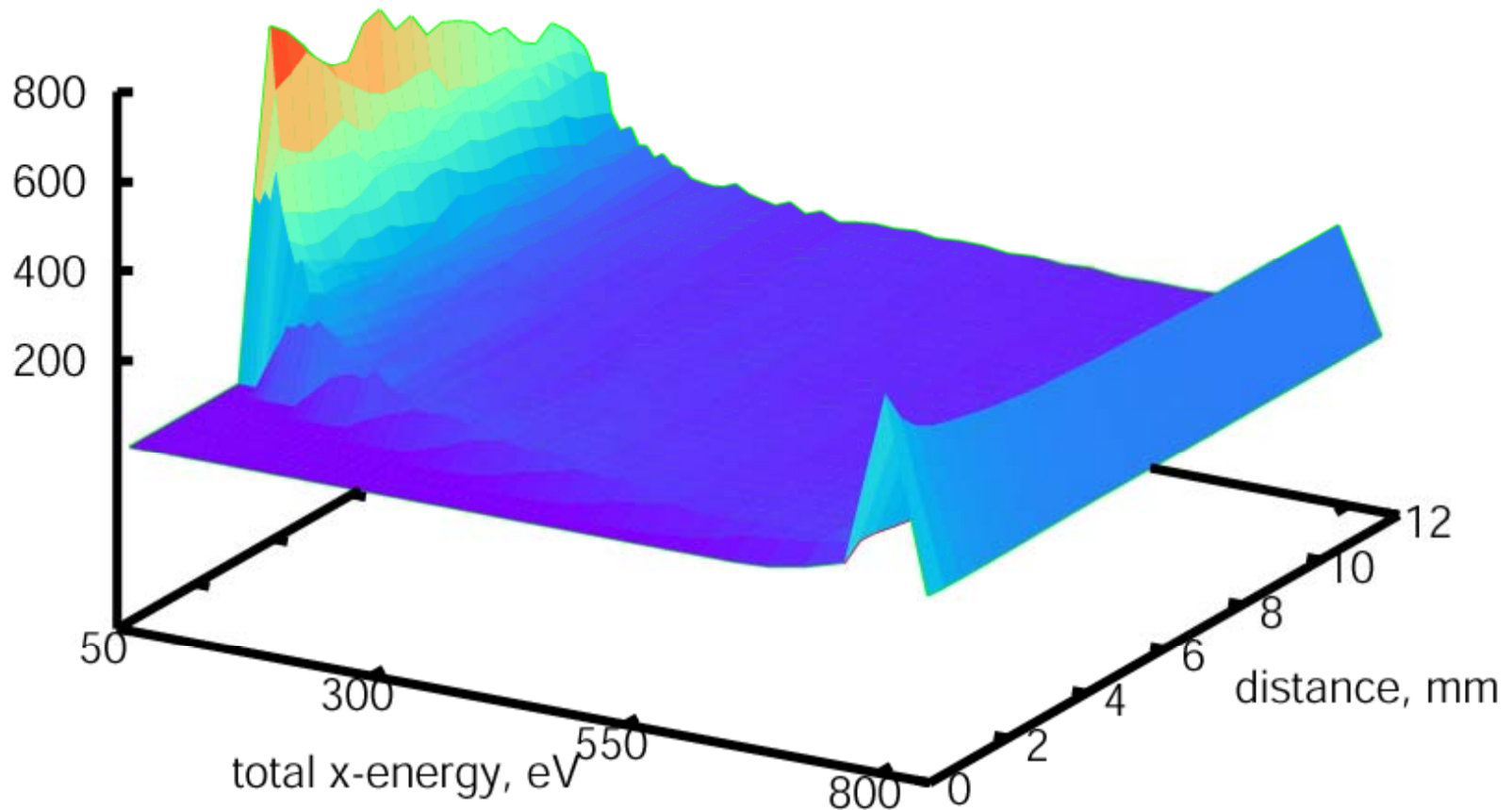


Anisotropic velocity distribution in the cathode fall, showing the primary beam and the avalanche

Using EDIPIC to simulate cold cathode DC discharge in helium

$U = 800$ V, $p = 3$ Torr, $L = 12$ mm

EVxDF, a.u.



Updated approximation for differential elastic scattering cross sections

EVDF is anisotropic => accurate modeling of scattering!

V. Vahedi and M. Surendra. CPC **87**, 179 (1995).

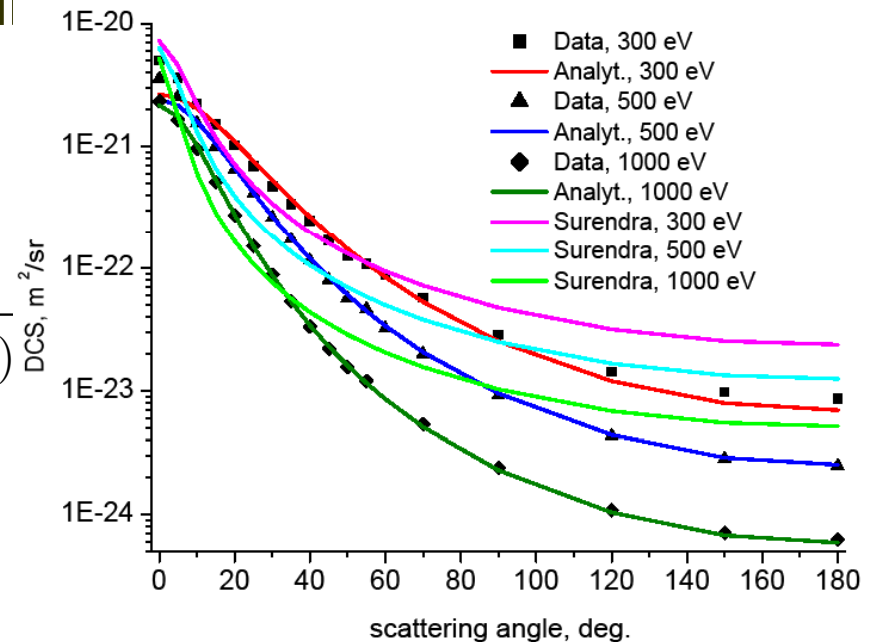
$$\frac{d\sigma(w, \chi)d\Omega}{\sigma_t(w)} = \frac{1}{4\pi} \frac{w}{\left[1 + w \sin^2(\chi / 2)\right] \ln(1 + w)}$$

Approximation by Phelps & Pitchford [1999], and Okhrimovsky et al. [2002]:

$$\frac{d\sigma(w, \chi)d\Omega}{\sigma_t(w)} = \frac{1}{4\pi} \frac{1 - \xi^2(w)}{\left[1 - \xi(w) + 2\xi(w) \sin^2(\chi / 2)\right]^2}$$

$$\xi(E) = 1 + \frac{p_1 x - p_2^2 - p_3}{(x - p_2)^2 + p_3} - \frac{p_1 x}{(x - p_4)^2 + p_5}, \quad x = \sqrt{E[\text{eV}]}$$

A. Khrabrov (2011).



Collective stopping and scattering of electron beams emitted from the walls

Electron beam propagating in plasma is subject to collective phenomena in weakly-collisional regime

Two-stream (bump on tail) instability

lead to beam scatter and energy relaxation

Nonlinear wave interaction with plasma electrons

yield plasma electron heating

Parametric instabilities and coupling to ions

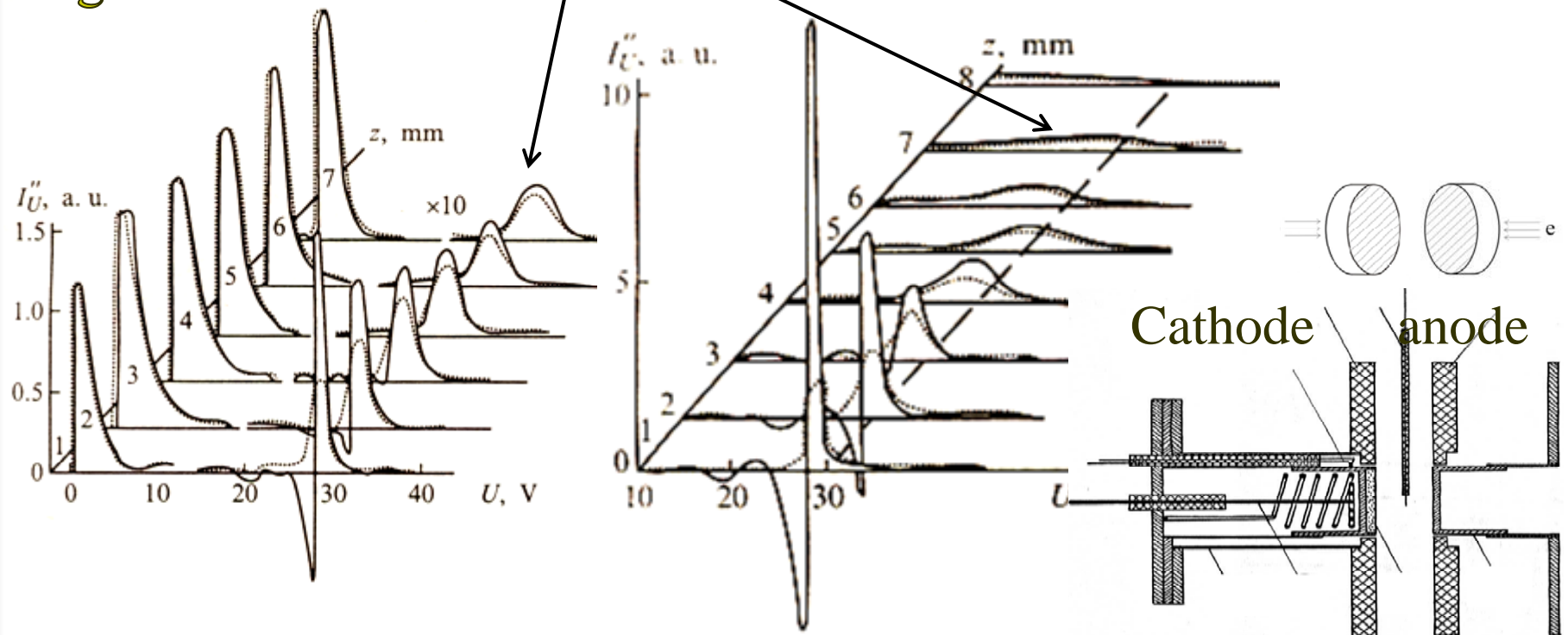
yield plasma ion heating

Measurements of Spatial Relaxation of Electron Beam Using Flat Probe

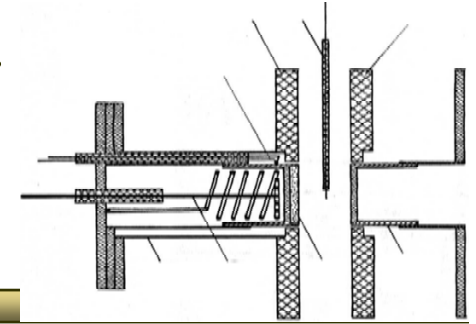
Evolution of the profile along the discharge axis in a collision-dominated plasma for $p_{\text{He}} = 2$ torr, $d = 1.2$ cm, $U_a = 29$ V; mean free path 2.5 mm,
 Left $j_s = 0.14$ A cm⁻² Right $j_s = 0.8$ A cm⁻²

Mustafaev, et al. (2001)

Observe large energy loss at higher current at 7 mm



Measurements of Spatial Relaxation of Electron Beam Using Flat Probe



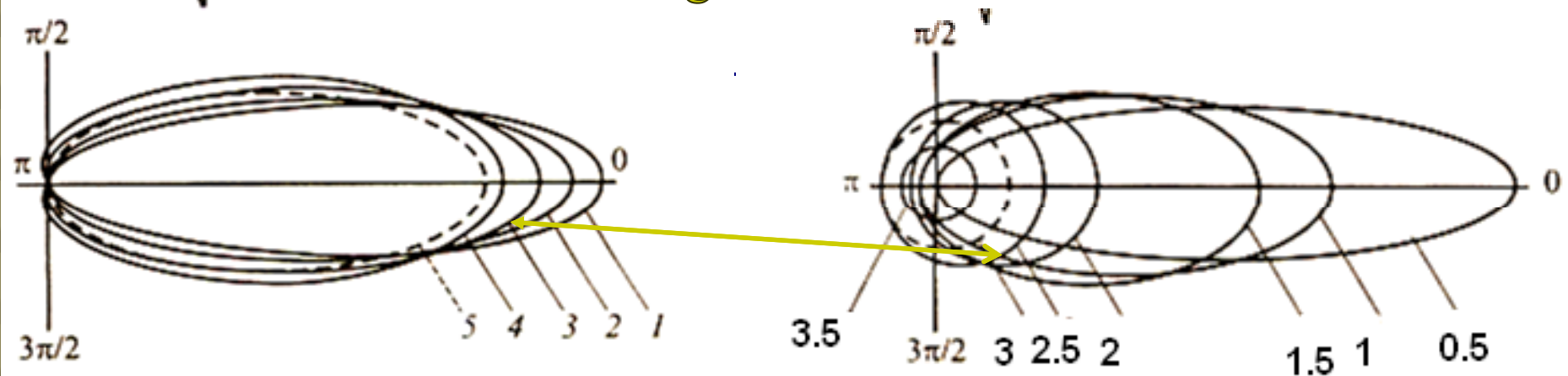
Evolution of the polar diagrams of the beam electrons along the discharge axis of beam electrons in a collisionless plasma for $p_{\text{He}} = 0.5$ Torr, $d = 0.6$ cm, numbers correspond to distance in mm from the cathode, the mean free path, $l_0 = 1$ cm,

current density, density of cold electrons and beam electrons

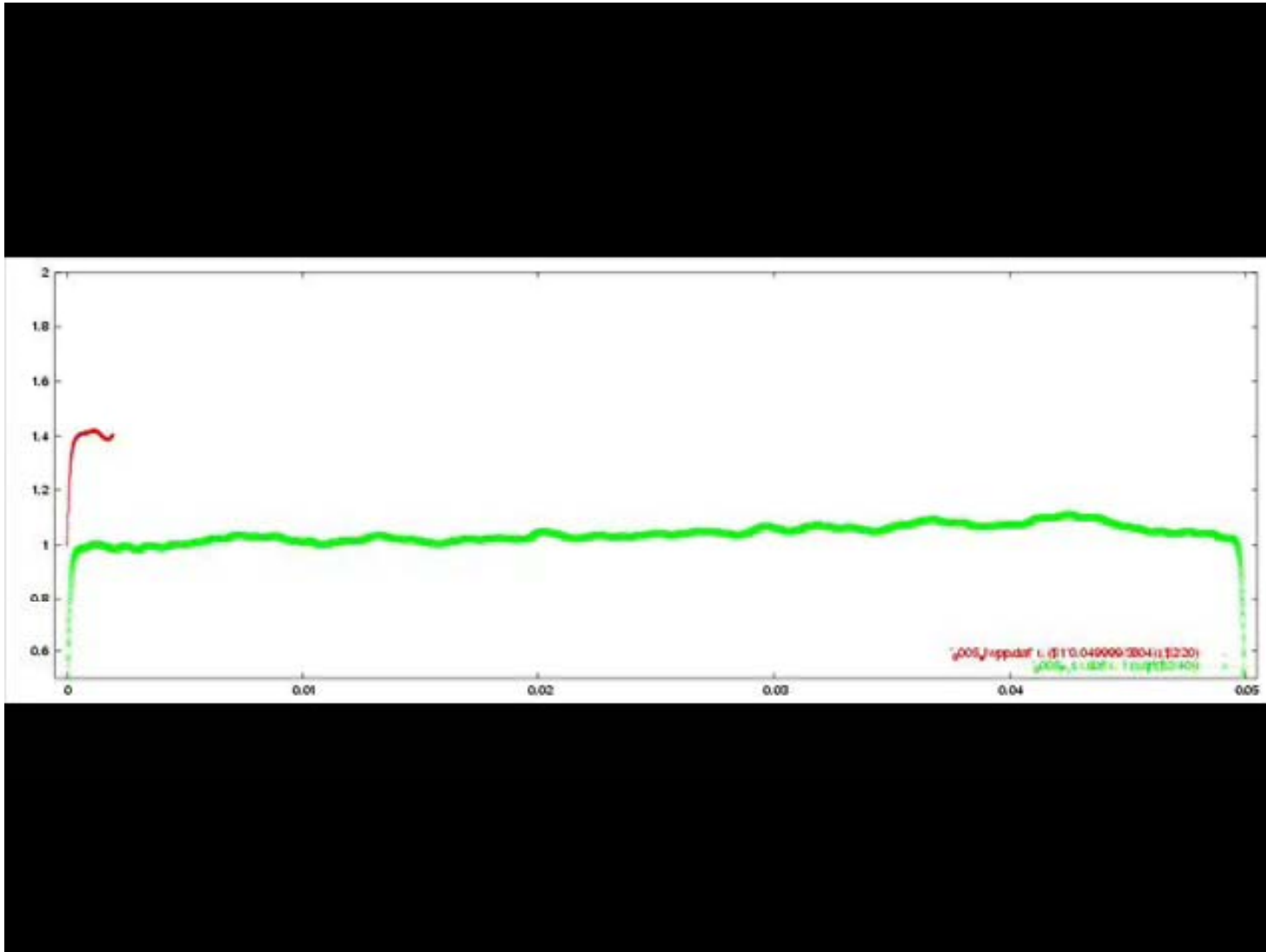
Left: $j_s = 0.1 \text{ A cm}^{-2}$, $n_t = 6.7 \times 10^{10} \text{ cm}^{-3}$, and $n_0 = 9 \times 10^9 \text{ cm}^{-3}$

Right: $j_s = 0.5 \text{ A cm}^{-2}$, $n_t = 2.8 \times 10^{11} \text{ cm}^{-3}$, and $n_0 = 6 \times 10^{10} \text{ cm}^{-3}$

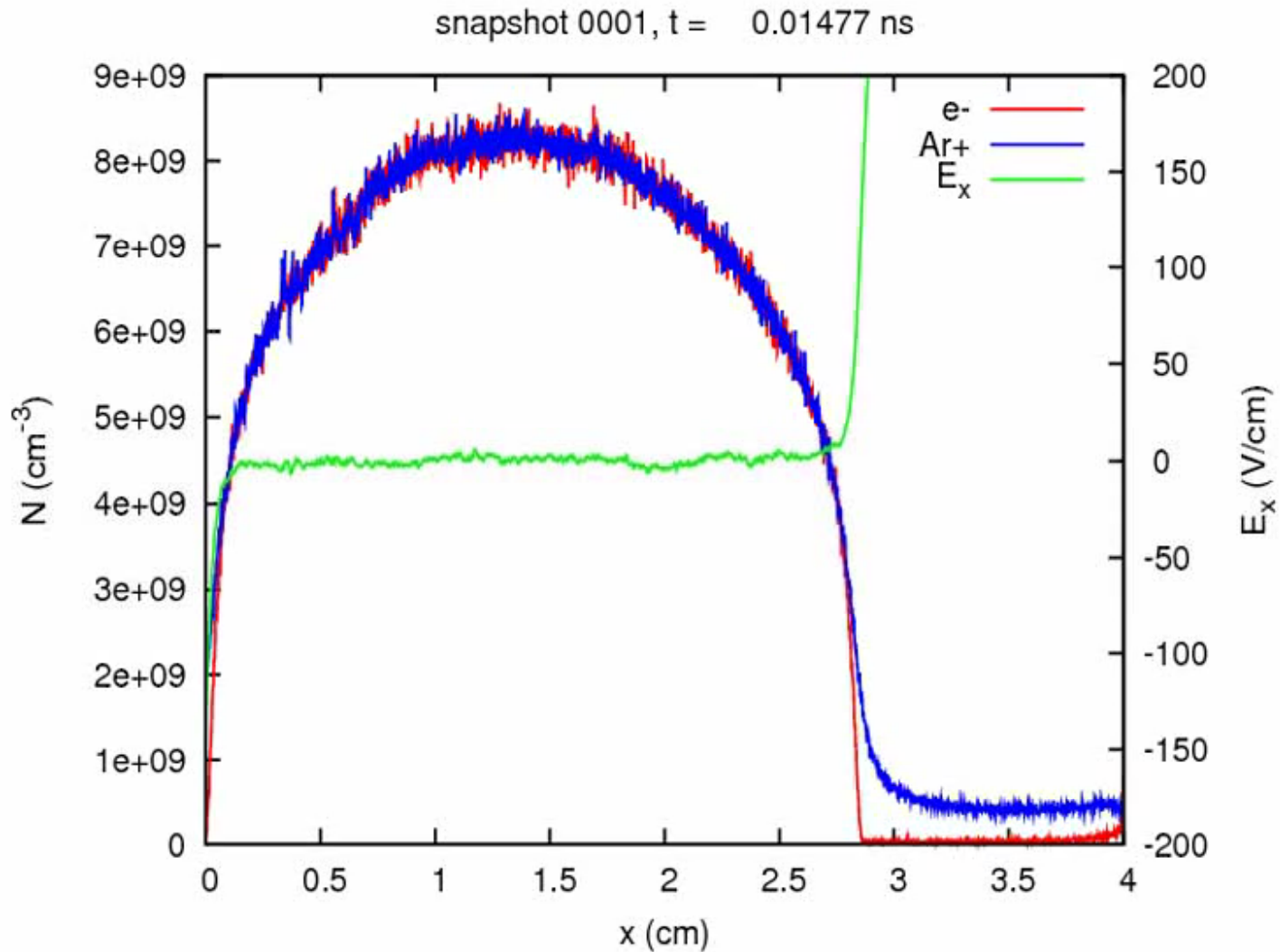
Observe big difference at 3 mm



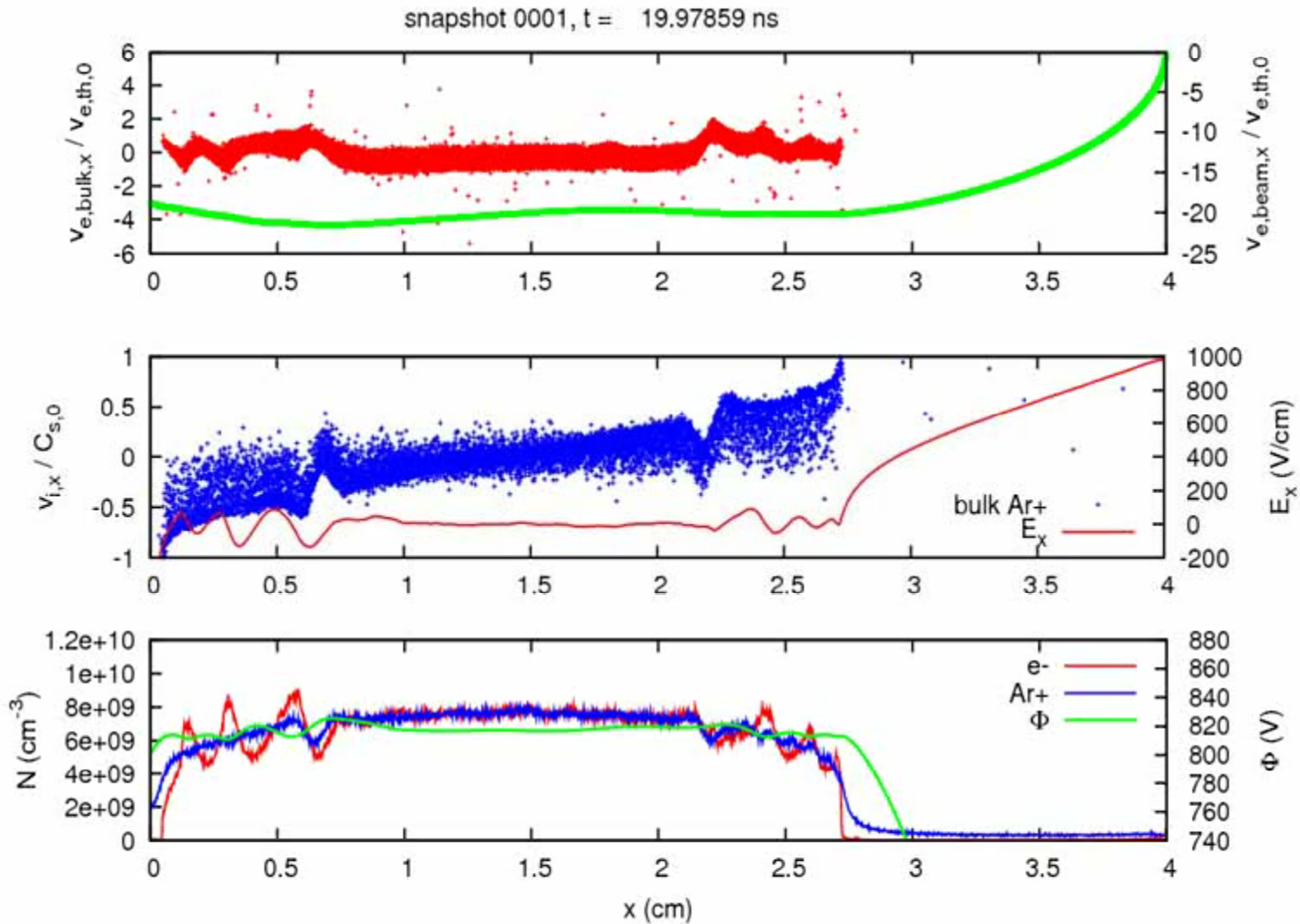
Simulation of two stream instability of 8eV beam, EDIPIC code by D. Sydorenko



Simulation of two stream instability of 800eV beam, EDIPIC code by D. Sydorenko



Simulation of two stream instability of 800eV beam, EDIPIC code by D. Sydorenko



Conclusions

Electron energy distribution function in low temperature plasmas is typically non-Maxwellian and even anisotropic in collisionless limit; beams can interact with plasma in collective processes; discharge modeling has to be done kinetically.

These non-equilibrium conditions provide considerable freedom to choose optimal plasma parameters for applications, which make gas discharge plasmas remarkable tools for a variety of plasma applications.

Specific examples include rf discharges, dc discharges with auxiliary biased electrodes for plasma control, Hall thruster discharges, and the cathode fall region of dc discharges.

Conclusions

- **Effect:**

- Explosive generation of cold electrons with power increase in capacitively coupled discharges and new two kinetic modes in molecular gases.
- Strong modification of electron energy distributions due to bounce resonance effect.
- Formation of anisotropic EVDF.
- Collective stopping and scattering of electron beams emitted from the walls.

- **Application:**

- Optimization of silane and methane discharges.
- Optimization of dual frequency CCP discharge with enhanced ionization and excitation.
- Enhanced etching.
- Plasma heating by beams to be avoided if needed by judiciously choosing plasma parameters.